# Supporting Information

## Wang et al. 10.1073/pnas.0911517107

### SI Text

**Cellular Elastic Model.** The total elastic energy ($U$) of an *Escherichia coli* cell under a bending force can be written as:

$$U = 2U_{\mathrm{MreB}} + U_0, \quad \textbf{[S1]}$$

where $U_{\mathrm{MreB}}$ is the elastic energy in a single MreB helical bundle, and $U_0$ is the elastic energy in the cell wall and the other mechanical components. The coefficient 2 comes from the fact that MreB has been shown to form a double-helix in *E. coli* (1). As the stuck part of the cell does not contribute to the elastic energy, we only consider the free part of the cell in our model.

We model the cell as an elastic rod:

$$U = \frac{1}{2}A\int_0^L \kappa^2 ds, \quad \textbf{[S2]}$$

$$U_0 = \frac{1}{2}A_0\int_0^L \kappa^2 ds, \quad \textbf{[S3]}$$

where $A$ is the flexural rigidity of the whole cell, $A_0$ is the flexural rigidity after A22 treatment, $L$ is the length of the free end, $\kappa$ is the local change in curvature of the cell during bending, and $s$ is the arc length along the cell. We have

$$\kappa = \frac{F}{A}(L - s). \quad \textbf{[S4]}$$

where $F$ is the bending force (2).

To investigate the effect of linking the MreB helix to the cell wall on bending stiffness, we considered two extreme assumptions that either the MreB bundle is tightly linked to the cell wall with infinite stiffness or that there is no linkage between the MreB bundle and the cell wall. Under the first assumption, cell bending leads to bending of the MreB bundle, the elastic energy of which is denoted as $U_{\mathrm{MreB,bending}}$. In addition, the bundle on one side the cell will be locally stretched, and the bundle on the other side will be locally compressed. The elastic energy due to these conformational changes is denoted $U_{\mathrm{MreB,stretching}}$. The total elastic energy of the bundle is then:

$$U_{\mathrm{MreB}} = U_{\mathrm{MreB,bending}} + U_{\mathrm{MreB,stretching}}. \quad \textbf{[S5]}$$

The bending energy is given by

$$U_{\mathrm{MreB,bending}} = \frac{1}{2}A_{\mathrm{MreB}}\int_0^{L'} \kappa'^2 ds', \quad \textbf{[S6]}$$

where $A_{\mathrm{MreB}}$ is the flexural rigidity of the MreB bundle, $L'$ is the length of the bundle, $\kappa'$ is the local curvature change of the bundle during bending, and $s'$ is the arc length along the helical bundle. We model the MreB bundle as a solid cylinder with radius $a$ and Young's modulus $E_{\mathrm{MreB}}$, thus

$$A_{\mathrm{MreB}} = \frac{1}{4}\pi a^4 E_{\mathrm{MreB}}. \quad \textbf{[S7]}$$

Because of MreB's helical conformation, $L'$ is related to $L$ by the equation:

$$\frac{L'}{L} = \frac{\sqrt{p^2 + (2\pi R)^2}}{p}, \quad \textbf{[S8]}$$

where $p$ is the pitch of the MreB helix and $R$ is the radius of the cell. Similarly,

$$\frac{s'}{s} = \frac{\sqrt{p^2 + (2\pi R)^2}}{p}. \quad \textbf{[S9]}$$

The coordinates of the helix before ($\mathbf{r_0}$) and after ($\mathbf{r}$) bending can be written as

$$\mathbf{r_0} = \left(R\cos\left(\frac{2\pi s}{p}\right), R\sin\left(\frac{2\pi s}{p}\right), s\right), \quad \textbf{[S10]}$$

$$\mathbf{r} = \left(R\cos\left(\frac{2\pi s}{p}\right), R\sin\left(\frac{2\pi s}{p}\right) + \Delta y, s\right), \quad \textbf{[S11]}$$

where $\Delta y$ is the displacement of the cell during bending along the cell's arc length ($s$):

$$\Delta y = \frac{F}{A}\left(\frac{Ls^2}{2} - \frac{s^3}{6}\right). \quad \textbf{[S12]}$$

$\kappa'$ is then given by

$$\kappa' = \left\|\frac{d^2\mathbf{r}}{ds'^2}\right\| - \left\|\frac{d^2\mathbf{r_0}}{ds'^2}\right\|. \quad \textbf{[S13]}$$

We also have

$$U_{\mathrm{MreB,stretching}} = \frac{1}{2}E_{\mathrm{MreB}}\pi a^2\int_0^{L'}\left(\left\|\frac{d\mathbf{r}}{ds'}\right\| - 1\right)^2 ds'. \quad \textbf{[S14]}$$

If we assume that the MreB bundle is tightly linked to the cell wall, Eqs. **S5–S14** and the parameters listed in Table S2 allow us to calculate the effect of A22 on cell bending stiffness. Using several combinations of the different values of the MreB bundle pitch and protein abundance taken from the literature, we estimate that for the tightly linked bundle, the addition of A22 causes a decrease in stiffness of 96.2 to 99.7% (Table S3).

Under the second assumption, that there is no linkage between the MreB bundle and the cell wall, cell bending leads to bending but not stretching of the MreB bundle:

$$U_{\mathrm{MreB}} = U_{\mathrm{MreB,bending}}. \quad \textbf{[S15]}$$

If we neglect the shearing movement of the MreB helix along the arc length of the cell, the position of the helix after bending can still be expressed by Eq. **S11**. Using Eqs. **S6–S13** and **S15**, and the parameters in Table S2, we predict a 0.00002% to 0.06% decrease in stiffness upon the addition of A22 (Table S3). If we had not neglected the shearing motion of the MreB helix along the cell cylinder, the helix would further relax, leading to smaller curvature change and less stored elastic energy. As a result, the true percentage would be even smaller than the calculated value above.

1. Vats P & Rothfield L (2007) Duplication and segregation of the actin (MreB) cytoskeleton during the prokaryotic cell cycle. *Proc Natl Acad Sci USA* 104:17795–17800
2. Landau LD & Lifshitz EM (1986) *Theory of Elasticity* (Pergamon Press, Oxford; New York) 3rd Ed.
3. Baba T et al. (2006) Construction of *Escherichia coli* K-12 in-frame, single-gene knockout mutants: The Keio collection. *Mol Syst Biol* 2(2006.0008).
4. Kruse T et al. (2006) Actin homolog MreB and RNA polymerase interact and are both required for chromosome segregation in *Escherichia coli*. *Gen Dev* 20:113–124.
5. Vats P, Shih YL, & Rothfield L (2009) Assembly of the MreB-associated cytoskeletal ring of *Escherichia coli*. *Mol Microbiol* 72(1):170–182.
6. Kruse T, Moller-Jensen J, Lobner-Olesen A, & Gerdes K (2003) Dysfunctional MreB inhibits chromosome segregation in *Escherichia coli*. *EMBO J* 22(19):5283–5292.
7. Karczmarek A et al. (2007) DNA and origin region segregation are not affected by the transition from rod to sphere after inhibition of *Escherichia coli* MreB by A22. *Mol Microbiol* 65(1):51–63.
8. van den Ent F, Amos LA, & Lowe J (2001) Prokaryotic origin of the actin cytoskeleton. *Nature* 413:39–44.
9. Kojima H, Ishijima A, & Yanagida T (1994) Direct measurement of stiffness of single actin filaments with and without tropomyosin by in vitro nanomanipulation. *Proc Natl Acad Sci USA* 91:12962–12966.

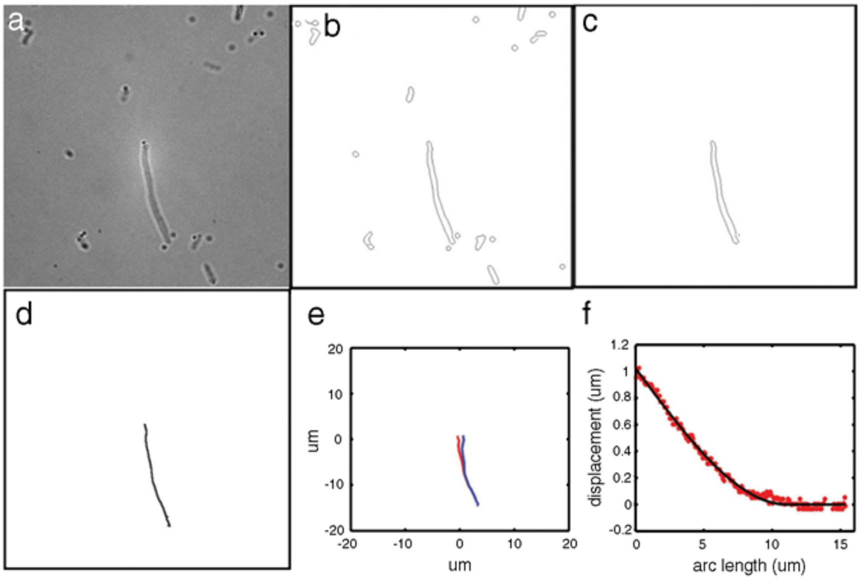


**Fig. S1.** The image analysis algorithm. (*A*) Typical DIC image of a cell. (*B*) The edge of the cell was extracted by the MATLAB Canny edge detector. (*C*) An area of interest was manually chosen to remove the other objects in the image. (*D*) By averaging the edge along the major axis of the cell, we got the cell's center line. (*E*) The original center line of the cell (*Red*) and the center line of the same cell under a bending force (*Blue*). (*F*) The displacement of the center line was fit to the theoretical shape of a bent elastic rod with a stuck end.

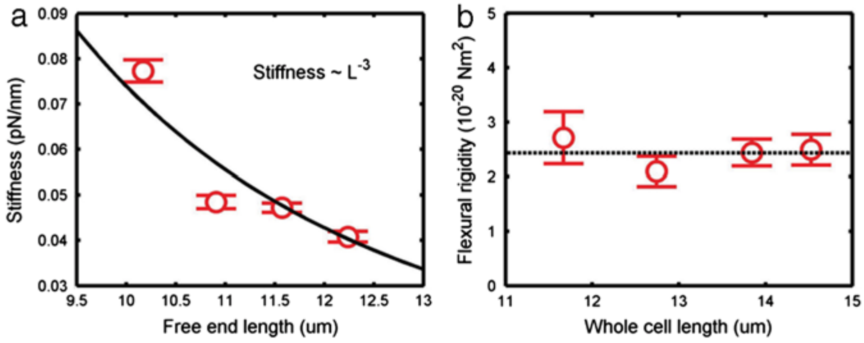


**Fig. S2.** The stiffness and flexural rigidity of a single cell during prolonged growth. (*A*) The stiffness versus the free end length (*L*). (*B*) The flexural rigidity versus the whole cell length. Strain: WX7 (Δ*ftsZ*)/λGL100 (*Plac::ftsZ*). Error bars indicate 95% confidence intervals.

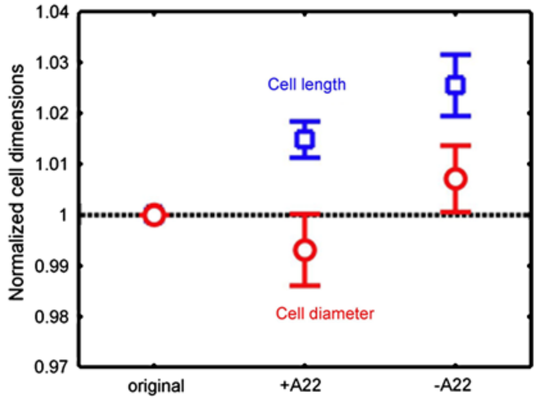


**Fig. S3.** The changes in cell length and diameter during the bending experiment. Strain: BW25113 *motA* <> *Amp*$^R$/ pWR20. Error bars indicate standard errors.

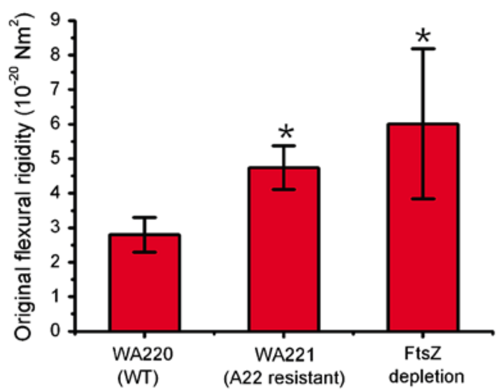


**Fig. S4.** Flexural rigidity of the wild-type, A22-resistant and FtsZ-depleted strains. WT: WA220 (W3110 *zhc-12::Tn10 mreB+*) ($N = 10$). A22-resistant: WA221 (W3110 *zhc-12::Tn10 mreB221*) ($N = 10$). FtsZ-depletion: WX7 (*ΔftsZ*)/λGL100 (*Plac::ftsZ*) ($N = 3$). *: $p < 0.05$. **: $p < 0.01$.

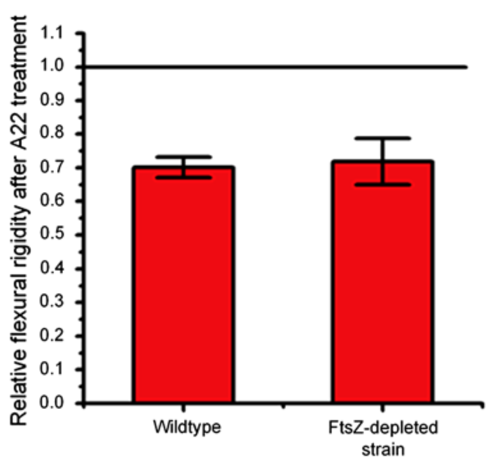


**Fig. S5.** The FtsZ-depleted cells show the same flexural rigidity decrease as the cephalexin-treated wild-type cells do after the addition of A22. Wild type: WA220 (W3110 *zhc-12::Tn10 mreB+*) ($N = 10$). FtsZ-depleted strain: WX7 (*ΔftsZ*)/λGL100 (*Plac::ftsZ*) ($N = 3$). Error bars indicate standard errors.

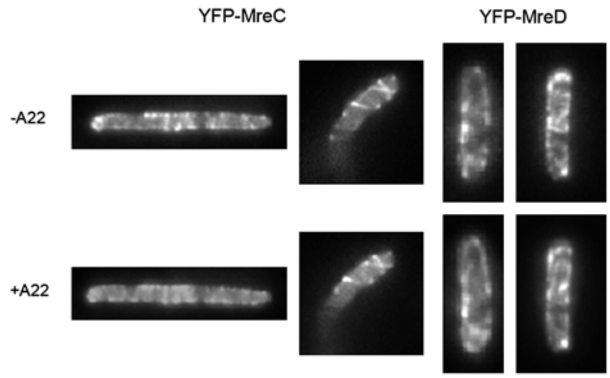


**Fig. S6.** MreCD localization is not affected by A22 on short time scales. YFP-MreC and YFP-MreD fusions were imaged before and 5 min after the addition of 10 μg/mL A22. The localization of these two proteins was not affected by the presence of the drug after 5 min. Strains: WA220/pVP1 (*Plac-yfp::mreC*) and WA220/pVP2 (*Plac-yfp::mreD*).

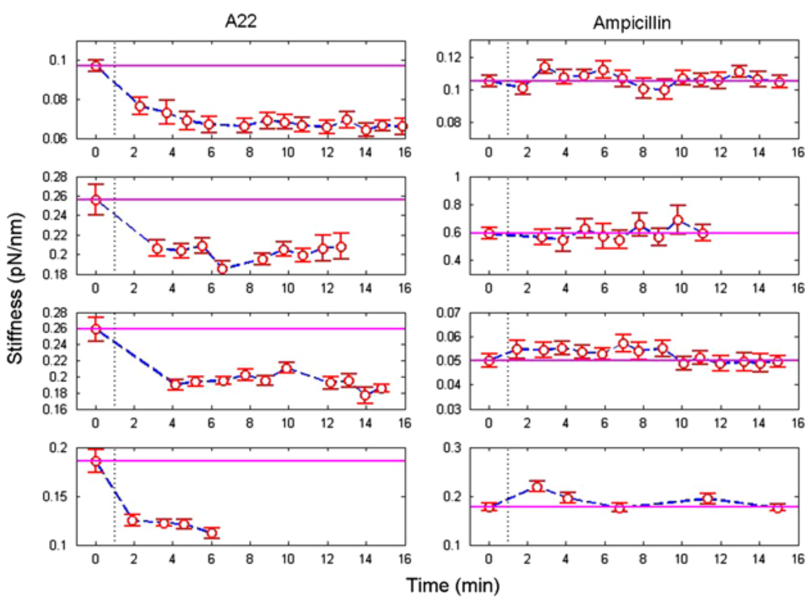


**Fig. S7.** The stiffness of single cells over time after the addition of A22 or ampicillin. The magenta lines indicate the initial stiffness. The black dotted lines show the time of A22 or ampicillin addition. Error bars indicate 95% confidence intervals. Strain: BW25113 *motA* <> *Kan*$^R$ (ampicillin sensitive).

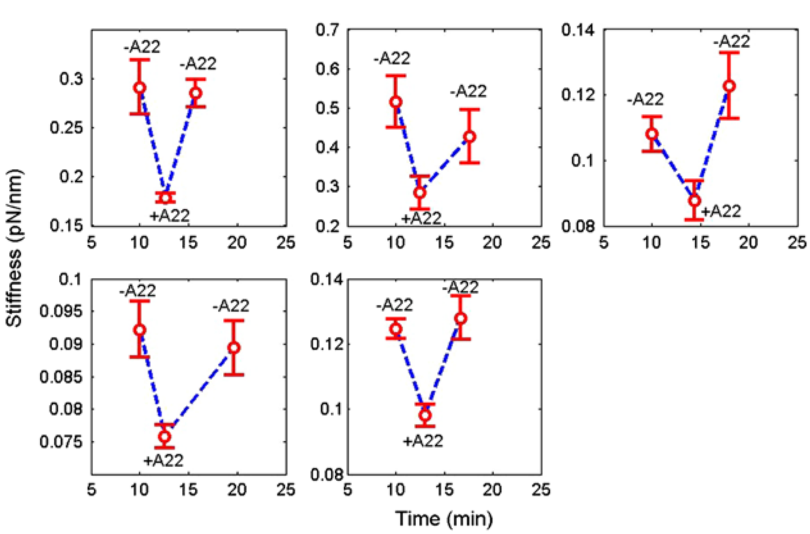


**Fig. S8.** Stiffness measurements of starved cells that were no longer growing. Error bars indicate 95% confidence intervals. Strain: BW25113 *motA* <> *Amp*$^R$/ pWR20.

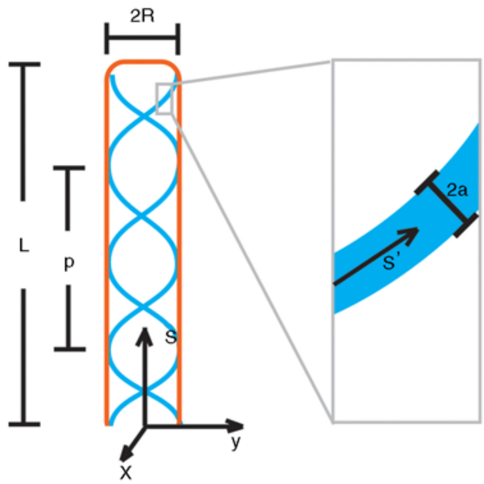


**Fig. S9.** Cellular elastic model. Orange: cell wall. Blue: MreB double helix. Only the free end of the cell is displayed.

**Table S1. Bacterial strain description**

| Strain/Plasmid/Phage | Characteristics | Citation/source |
|---|---|---|
| BW25113 *motA* <> *Kan*$^R$ | *rrnB3 ΔlacZ4787 hsdR514 Δ(araBAD)567 Δ(rhaBAD)568 rph-1 motA* <> *Kan*$^R$ | Baba et al. 2006 (3) |
| BW25113 *motA* <> *Amp*$^R$ | *rrnB3 ΔlacZ4787 hsdR514 Δ(araBAD)567 Δ(rhaBAD)568 rph-1 motA* <> *Amp*$^R$ | Baba et al. 2006 (3) but with *Kan*$^R$ replaced with *Amp*$^R$ |
| WA220 | W3110 *zhc-12::Tn10 mreB+* (A22 sensitive) | Kruse et al. 2006 (4) |
| WA221 | W3110 *zhc-12::Tn10 mreB221* (A22 resistant) | Kruse et al. 2006 (4) |
| WX7 | *Leu::Tn10 ΔftsZ trpE61 trpA62 tna-5 purB+ λ- minB+ dadR1* | Vats et al. 2007 (1) |
| pWR20 | Constitutively expressed EGFP, *Kan*$^R$ | A kind gift from William S. Ryu. |
| λGL100 | *Plac::ftsZ Amp*$^R$ | Vats et al. 2007 (1) |
| *pVP*1/2 | *Plac-yfp::mreC/D* | Vats et al. (2009) (5) |

**Table S2. Parameters in the cellular elastic model**

| No. | Name | Quantity | Citation/source |
|---|---|---|---|
| 1 | Cell radius (*R*) | 400 nm | This work |
| 2 | Normal cell length | 2 μm | This work |
| 3 | Pitch of MreB helix (*p*) | 0.5–2 μm | Kruse et al. 2003 (6) and Vats et al. 2007 (1) |
| 4 | MreB abundance | 15, 000–40, 000 molecules/cell | Kruse et al. 2003 (6) and Karczmarek et al. 2007 (7) |
| 5 | Diameter of MreB monomer | 5.1 nm | van den Ent et al. (2001) (8) |
| 6 | MreB bundle radius (*a*) | 5.6–16 nm | Calculated from the parameters above |
| 7 | Young's modulus of MreB (assumed to the be same as actin) | 2 GPa | Kojima et al. 1994 (9) |

**Table S3. The percentage of stiffness decrease based on alternative parameters**

| Quantities | Original | Lower MreB pitch | Reduced MreB concentration | Lower MreB pitch and reduced MreB concentration |
|---|---|---|---|---|
| Number of MreB per cell | 40,000 [Kruse (6)] | 40,000 [Kruse (6)] | 15,000 [Karczmarek (7)] | 15,000 [Karczmarek (7)] |
| MreB pitch (μm) | 2 [Vats (1)] | 0.5 [Kruse (6)] | 2 [Vats (1)] | 0.5 [Kruse (6)] |
| MreB bundle radius (nm) | 16 | 9.1 | 9.9 | 5.6 |
| Percentage of stiffness decrease with tight linkage | 99.73 ± 0.03% | 98.5 ± 0.2% | 99.30 ± 0.09% | 96.2 ± 0.6% |
| Percentage of stiffness decrease with no linkage | 0.064 ± 0.004% | 0.00015 ± 0.00002% | 0.0093 ± 0.0006% | 0.000021 ± 0.000003% |